ACS Chemical Neuroscience

Research Article

pubs.acs.org/chemneuro

ClC-3 Is an Intracellular Chloride/Proton Exchanger with Large Voltage-Dependent Nonlinear Capacitance

Raul E. Guzman,[†,‡] Matthias Grieschat,[†] Christoph Fahlke,*[,†,‡] and Alexi K. Alekov*[,†]

[†]Institut für Neurophysiologie, Medizinische Hochschule Hannover, D-30625 Hannover, Germany

[‡]Institute of Complex Systems, Zelluläre Biophysik, Forschungszentrum Jülich, 52425 Jülich, Germany

Supporting Information

ABSTRACT: The chloride/proton exchangers ClC-3, ClC-4 and ClC-5 are localized in distinct intracellular compartments and regulate their luminal acidity. We used electrophysiology combined with fluorescence pH measurements to compare the functions of these three transporters. Since the expression of WT ClC-3 in the surface membrane was negligible, we removed an N-terminal retention signal for standard electrophysiological characterization of this isoform. This construct ($ClC\text{-}3_{13-19A}$) mediated outwardly rectifying coupled Cl^-/H^+ antiport resembling the properties of ClC-4 and ClC-5. In addition, ClC-3 exhibited large electric capacitance, exceeding the nonlinear capacitances of ClC-4 and ClC-5. Mutations of the proton glutamate, a conserved residue at the internal side of the protein, decreased ion transport but increased nonlinear capacitances in all three isoforms. This suggests that nonlinear capacitances in mammalian ClC transporters are regulated in a similar manner. However, the voltage dependence and the amplitudes of these capacitances differed strongly between the investigated isoforms. Our results indicate that ClC-3 is specialized in mainly performing incomplete capacitive nontransporting cycles, that ClC-4 is an effective coupled transporter, and that ClC-5 displays an intermediate phenotype. Mathematical modeling showed that such functional differences would allow differential regulation of luminal acidification and chloride concentration in intracellular compartments.

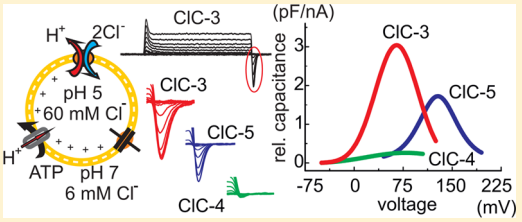

KEYWORDS: *ClC transport, ClC-3, nonlinear capacitance, synaptic acidification, endocytosis, gating currents*

ClC-3, ClC-4, and ClC-5 belong to the superfamily of CLC channels and transporters. The functional importance of these proteins has been established based on hereditary diseases and mouse models. They all reside in intracellular organelles and regulate luminal pH, but fulfill distinct physiological functions.[1] Within the nervous systems, ClC-3 is highly expressed in hippocampus[2] and regulates synaptic transmission and luminal pH in synaptic vesicles,[3,4] but the mechanisms of this regulation are still debated. *Clcn3* knockout mice undergo severe neurodegeneration,[3,5] but ClC-3 is also expressed in and might be involved in the volume regulation of heart muscle cells.[6,7] ClC-4 transport affects copper metabolism[8] and transferrin receptor function.[9] However, knockout of the *Clcn4* gene in mice does not produce a clear pathophysiological phenotype.[1] Mutations in *CLCN5* cause Dent's disease, a hereditary renal disorder.[10] Mouse model investigations show that knockout of ClC-5 results in impaired endocytosis, endosomal acidification, and vesicular chloride homeostasis.[11−14]

In contrast to the well established specialization of ClC-3, ClC-4, and ClC-5 in subcellular and tissue distribution, little is known about the possible functional differences between the isoforms. ClC-4 and ClC-5 mediate coupled Cl^-/H^+ exchange across biological membranes.[15,16] For ClC-4 and ClC-5, a sufficient fraction of transporters inserts into the surface membrane allowing the application of standard electrophysiological techniques for functional studies. In contrast, surface expression of ClC-3 is too low[17,18] to allow unambiguous characterization of its transport characteristics. A variety of very different functional phenotypes have been assigned to ClC-3. For example, ClC-3 was initially thought to be the molecular correlate of the volume activated anion conductance[19] observed in most mammalian cells. Later, ClC-3 was reported to represent a CamKII activated anion channel,[20] and recently (uncoupled) ClC-3 transport was linked to a proton activated anion conductance,[21,22] that is endogenous to a variety of mammalian cells.[23−26]

Many of the described ClC-3 currents were suspected to represent endogenous currents.[1] The persisting controversy surrounding the functional properties of ClC-3, thus, likely originates from the lack of unambiguous functional markers that can be used to separate the ClC-3 conductance from endogenous conductances. Recently, prominent gating currents and nonlinear capacitances that result from incomplete transport cycles and do not contribute to electrogenic Cl^-/H^+ antiport were described in ClC-5.[27−29] Capacitive gating currents are often observed in a variety of membrane ionic channels, motor proteins, transporters, and pumps,[30−34] and represent an important biophysical characteristic of these proteins. Here, we used this feature to separate ClC-3 transport

Received: January 30, 2013
Accepted: March 19, 2013
Published: March 19, 2013

 © 2013 American Chemical Society

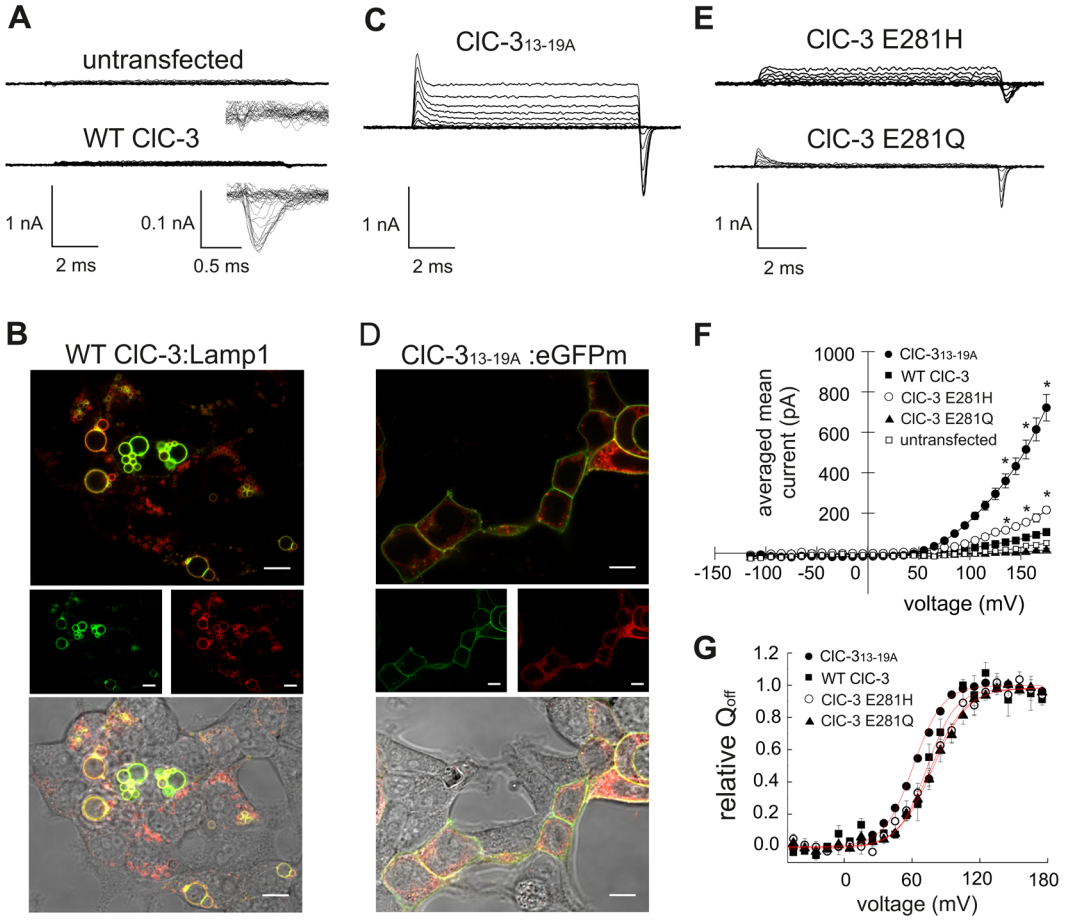

Figure 1. Cellular localization and functional properties of ClC-3. (a) Representative P/4 leak subtracted patch-clamp whole-cell recordings from an untransfected and a cell expressing WT ClC-3, elicited by voltage pulses between −115 and +175 mV. The insets show enlarged the capacitive currents at the end of the voltage pulse. (b) Confocal and DIC images of cells cotransfected with ClC-3 WT and the lysosomal marker protein Lamp-1. (c) Representative whole-cell recording from a cell expressing ClC-3_{13-19A}. (d) Confocal and DIC images of cells cotransfected with ClC-3_{13-19A} and the membrane marker EGFP-mem. (e) Representative whole-cell recording from cell expressing the proton glutamate mutations ClC-3 E281Q and ClC-3 E281H. (f) Mean current amplitudes versus voltage for cells expressing WT and various mutant ClC-3 constructs obtained from recordings as shown in (a), (c), and (e) (ClC-3_{13-19A} n = 12 and ClC-3 WT n = 8, ClC-3 E281Q n = 6, ClC-3 E281H n = 5, untransfected n = 7). Significantly different current amplitudes are marked with a star. (g) Voltage dependence of the apparent gating charge movements for WT and various mutant ClC-3 constructs obtained from integrating the surface under the nonlinear capacitive currents at the end of the voltage steps. Lines represent nonlinear fits to the data with standard Boltzmann function. Summarized fit parameters are enlisted in Table 1.

from other conductances. This allowed us to provide the, to our knowledge, first unambiguous functional description of this isoform as Cl^-/H^+ exchanger. As a consequence, we were able to directly compare the properties of the three mammalian ClC transporters ClC-3, ClC-4 and ClC-5 and to demonstrate that they exhibit pronounced functional specializations.

RESULTS

Heterologous Expression and Functional Properties of ClC-3. Whole cell recordings of cells transfected with WT ClC-3 yielded only very small ionic currents (Figure 1a, f), as expected form the predominant intracellular localization of the protein (Figure 1b). The fluorescence pattern of ClC-3-mRFP overlapped, as demonstrated before,[35] with coexpressed Lamp-1-YFP, a specific lysosomal marker.[36] However, closer observation of leak subtracted current traces revealed that in contrast to untransfected cells, cells expressing WT ClC-3 exhibited small but pronounced capacitive transients upon depolarizing voltages (Figure 1a). Integrating the area under the capacitive transients provided the apparent charge moved across the transmembrane electric field and revealed Boltzmann-type voltage dependence for ClC-3 (Figure 1g). Based on these findings, we considered the possibility that the capacitive transients in transfected cells are mediated by voltage-dependent gating transitions in ClC-3.

To test this hypothesis, we performed two different experiments. Mutations of the so-called proton glutamate E268, a conserved residue at the intracellular side of the protein,[37,38] dramatically increased the magnitude of the ClC-5 capacitive currents[27,28] (Supporting Information Figure S1). We therefore introduced the analogous mutations into ClC-3 that completely (E281Q) or partially (E281H) prevent protonation of the side chain at this position and observed much larger capacitive currents (Figure 1e) with voltage dependence that closely resembles the voltage dependence of the gating charges observed in WT ClC-3 (Figure 1g). Moreover, cells transfected with the "partially competent" mutant E281H ClC-3 [28] exhibited at depolarized voltages also conductances, significantly larger than in untransfected cells (Figure 1f), suggesting that WT ClC-3 also mediates electrogenic transport.

dx.doi.org/10.1021/cn400032z | ACS Chem. Neurosci. 2013, 4, 994−1003

Table 1. Voltage Dependence of ClC-3, ClC-4, and ClC-5[a]

cell expressing		ClC-3	ClC-3_{13-19A}	ClC-4	ClC-5
WT	$V_{0.5}$ (mV)	74.8 ± 2	61 ± 1	78 ± 7	129 ± 2
	z (e_0)	−1.7 ± 0.1	−1.1 ± 0.1	−1.0 ± 0.1	−1.3 ± 0.1
	n	5	12	8	7
E281H/E268H	$V_{0.5}$ (mV)	77.8 ± 2	89 ± 2	90 ± 2	121 ± 1
	z (e_0)	−1.7 ± 0.2	−1.1 ± 0.1	−1.1 ± 0.1	−1.3 ± 0.1
	n	5	14	8	6
E281Q/E268Q	$V_{0.5}$ (mV)	80.5 ± 3	61 ± 1	81 ± 1	109 ± 1
	z (e_0)	−1.6 ± 0.1	−1.2 ± 0.1	−1.1 ± 0.1	−1.4 ± 0.1
	n	6	8	7	7

[a]Fit parameters describing the voltage dependence of the off-gating charges or nonlinear capacitances for various constructs. $V_{0.5}$ represents the half-maximal voltage of activation, the charge (z) denotes the apparent number of elementary charges (e_0) displaced over the membrane electric field, and n denotes the number of cells.

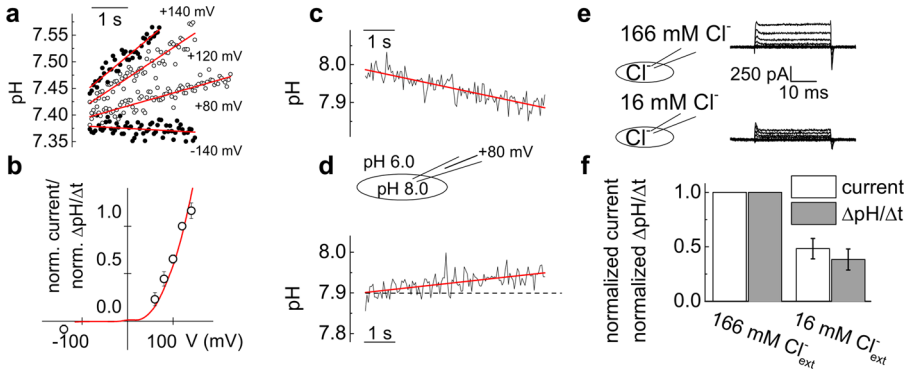

Figure 2. Transport properties of ClC-3_{13-19A}. (a) Representative voltage-dependent changes of internal pH in cells expressing ClC-3_{13-19A}. Lines represent linear fits to the data. (b) Summarized rates of intracellular pH changes ($\Delta pH/\Delta t$) plotted against the voltage (ClC-3_{13-19A}, $n = 6$). The rates were obtained from the slope of the linear fits in (a). Red line represents the current−voltage dependence of the ionic currents for the cell depicted in (a). (c) Representative recording demonstrating the acidification in untransfected cells upon inward directed transmembrane proton gradient. The experimental conditions are schematically depicted between panels (c) and (d); the internal [Cl^-] was reduced in these experiments to 10 mM. (d) Representative recording of alkalinization in HEK293T cells expressing ClC-3_{13-19A} demonstrating the transport of protons against their diffusion gradient ($n = 5$). The dashed line visualizes the zero-slope behavior. (e) Schematic representation of the experimental ionic conditions and representative recordings in HEK293T cells expressing ClC-3_{13-19A} elicited with 30-ms pulses with voltages between −115 and +135 mV. Cells were perfused sequentially with external solution containing 166 mM [Cl^-] (upper part) and 16 mM [Cl^-] +150 mM [gluconate$^-$] (lower part). (f) Ionic transport at +135 mV (steady-state current) and rates of intracellular alkalinization ($\Delta pH/\Delta t$) at +120 mV for the conditions depicted in (e) and normalized to the corresponding value measured at 166 mM. Data were obtained from cells sequentially perfused with both external solutions ($n = 6$).

Apart from increasing the amplitudes of nonlinear capacitances (Figure 1e), we set out to improve the plasma membrane density of ClC-3. Recently, a dileucine acidic cluster was identified as retention signal and its removal shown to permit surface membrane insertion. [18] We drew on this finding and mutated all amino acids in the cluster to alanine. For conciseness, we will henceforth refer to this construct as ClC-3_{13-19A}. ClC-3_{13-19A} partially colocalized with pEGFP-mem, a plasma membrane marker (Figure 1d) and mediated much larger outwardly rectifying ionic currents (Figure 1c, 1f) resembling ClC-4 and ClC-5 transport investigated under the same experimental conditions.[28,39] Again, an integration of the surface under the off-gating capacitive currents provided the voltage dependence of the gating charge which was similar to the one obtained for WT ClC-3, but also for the mutants E281H and E281Q ClC-3 (Figure 1g). There were no differences in the apparent electric charge moved during the transition and only moderate differences in the midpoint of activation of the gating charge movements (Figure 1g, Table 1). We encountered slightly slower off-gating charge kinetics for WT and E281H ClC-3 (Figure 1a and 1d) than for ClC-3_{13-19A} and E281Q ClC-3 We believe that this apparent change in kinetics is due to the small amplitude of these signals. The superposition of random noise and gating charge movements obscures the real time course of the traces. This is a common problem associated with the P/N leak-subtraction procedures that obligatory increase the noise-to-signal ratio of the recordings. We concluded therefore that the major effect of the 13−19A amino acid substitution in ClC-3_{13-19A} is an increase in the surface abundance of ClC-3.

ClC-3 Mediates Coupled Anion/Proton Antiporter with Unitary Transport Rates Similar to ClC-4 and ClC-5. The ionic currents mediated by ClC-3_{13-19A} are large enough to permit reliable investigation of the transport properties of ClC-3. It is well established that ClC-4 and ClC-5 mediate coupled anion/proton antiport.[15,16] We therefore performed simultaneous voltage-clamp and fluorescence pH measurements in transfected cells, a methodology that we have previously applied to describe ClC-4 and ClC-5 transport.[28,39] Upon depolarization, significant alkalinization was observed in cells expressing ClC-3_{13-19A} (Figure 2a). The observed pH changes and the current amplitudes demonstrated closely similar voltages dependence and rectification (Figure 2b), suggesting that they reflect thermodynamically coupled trans-

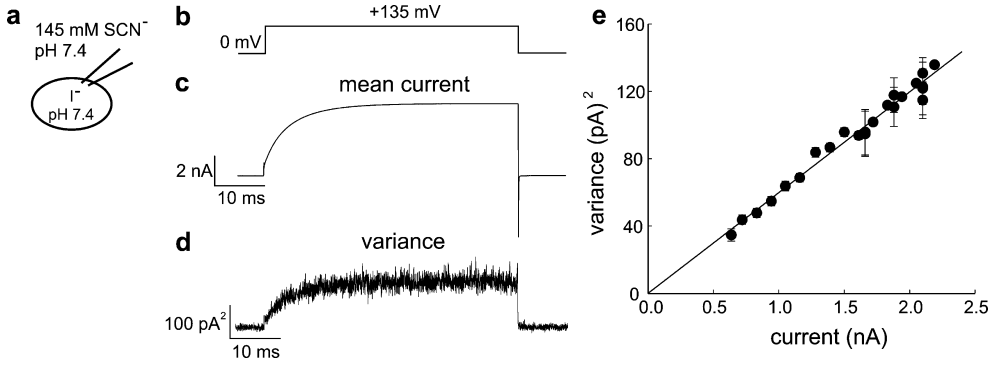

Figure 3. Variance analysis of $ClC3_{13-19A}$. (a) Schematic representation of the experimental ionic conditions. (b) Voltage protocol applied to activate ClC-3_{13-19A}. The data were acquired at +135 mV after filtering with 10 kHz Butterworth filter and digitization at 100 kHz. (c) Mean current obtained by averaging 300 current traces. (d) Calculated current variance for the cell depicted in (c). (e) Variance-current plot for ClC-3_{13-19A} for the cell presented in (c) and (d). Line represents fit with a parabolic equation to the data.

port. To provide further evidence that ClC-3 mediates coupled anion/proton exchange, we investigated whether protons can be moved across the membrane against their electrochemical gradient. Measurements in untransfected HEK293T cells display relatively high proton permeability and cells perfused with a high-pH intracellular solution (pH 8) and subsequently exposed to a low-pH extracellular solution exhibited pronounced acidification (+80 mV, Figure 2c). However, significant alkalinization was observed under such conditions in cells expressing ClC-3_{13-19A}, upon depolarization to +80 mV (Figure 2d). This voltage is well below the equilibrium chemical potential for protons under these conditions,[41] suggesting that proton transport is coupled to the electrochemical gradient of other ions. Finally, we established that the rates of intracellular pH changes are reduced upon reduction of the external Cl^- concentration (Figure 2e and f) showing that ClC-3 proton transport is coupled to the electrochemical gradient of Cl^-.

We next performed nonstationary noise analysis[42] with SCN^- in the bath solution, a condition that was previously reported to uncouple anion from proton transport[43] and to result in a channel-like behavior in mammalian ClC transporters.[39] In addition, we used intracellular I^- to slow down the time course of activation and increase the resolution of the analysis.[44] The current variance of ClC-3_{13-19A} varied with the amplitude of the ionic current (Figure 3b). The slope of the current-variance plot (Figure 3c), which corresponds to the unitary transport current, provided a value of 80 ± 10 fA (n = 6) for ClC-3_{13-19A}. Similar values were reported previously for the two other isoforms ClC-4 and ClC-5.[28,38,39,44] Nonstationary noise analysis can also be used to determine the number of proteins in the membrane and the apparent open probability of the investigated channels.[45] Unfortunately, in the case of ClC-3, the current variances depended linearly on the current amplitudes (Figure 3c). Such behavior is characteristic for channels, with very low open probability, and prevents the accurate determination of the number of proteins.[46] Translating this finding to the voltage-dependent behavior of ClC transporters, these findings suggest that ClC-3 exhibits a low overall transport probability, that is, that the probability that a ClC-3 protein mediates a transporting cycle associated with ion transport is low.

The robust expression of ClC-3_{13-19A} also permitted repetition of previous pharmacological tests. ClC-3 was reported to be blocked by MTSES.[21] We repeated this experiment but did not observe any modification (Supporting Information Figure S2).

Quantitative Description of Nonlinear Capacitances in ClC-3. ClC-3 differs from ClC-4 and ClC-5 in the prominent capacitive peaks observed at beginning and end of applied voltage steps (Figures 1 and 4a). We quantified and compared the ratio between capacitive charge movements and transport currents in the different isoforms. For this purpose we used lock-in impedance analysis that revealed large bell-shaped voltage-dependent nonlinear capacitances for ClC-3_{13-19A} (Figure 4d, inset). Such capacitances have not been documented in untransfected cells but were previously reported for ClC-5[28] and we therefore decided to use them to additionally corroborate the specificity of the observed ClC-3 currents. To this end, we again mutated the so-called proton glutamate in ClC-3_{13-19A} (mutations E281H and E281Q). Similarly to the observations in ClC-5, these mutations increased the gating currents but reduced electrogenic transport (Figure 4a–c) without dramatically altering the voltage dependence of the nonlinear capacitance (see Table 1). Normalizing the nonlinear capacitances to the transport current at +135 mV revealed an inversely proportional dependence between these two parameters (Figure 4d). The surface area under the off-gating currents (enlarged in Figure 4a–c) yields the off-gating charge (Q_{off}) moved during the voltage dependent transition and is proportional to the nonlinear capacitance. For all constructs, Q_{off} was linearly proportional to the measured ionic current, with both parameters corresponding to the surface expression of the protein (Figure 4e). However, the slopes of the line differed for the different constructs. It is small for ClC-3_{13-19A} and very large for ClC-3_{13-19A} E281Q (Figure 4e). This phenotype is consistent with our findings on ClC-5 (Supporting Information Figure S1)[28] and provides additional evidence that the here described Cl^-/H^+ antiport and the nonlinear capacitances are mediated by ClC-3.

ClC-4 Also Exhibits Nonlinear Capacitances and Gating Charge Movements. In previous experiments, we could not detect gating currents in ClC-4.[39,40] We observed tiny capacitive transients (see Figure 5a); however, their small amplitudes made them hard to interpret. We mutated the proton glutamate in this isoform to histidine or glutamine (E281H and E281Q) (Figure 5b, c). The largest nonlinear capacitances and gating charge movements were observed for the glutamine mutant (E281Q) while mutation E281H that still

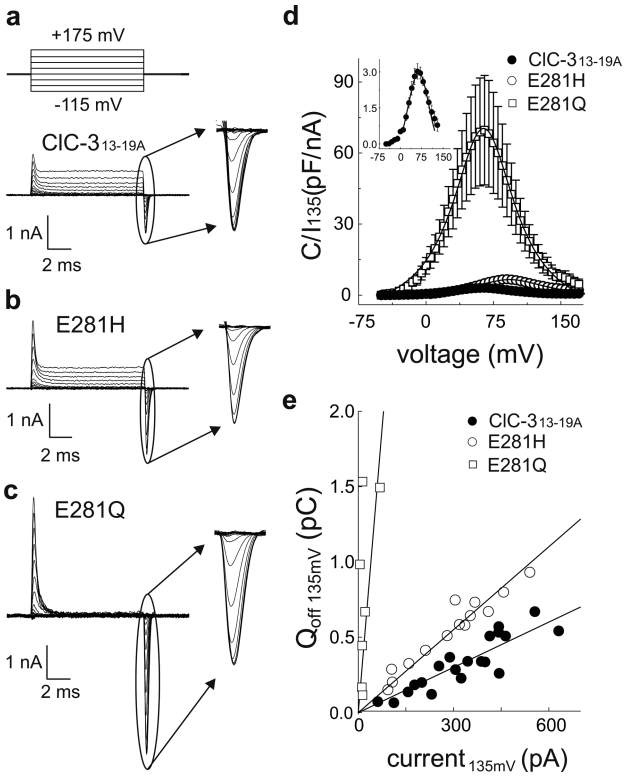

Figure 4. Proton glutamate E281 regulates transport and nonlinear capacitances in ClC-3. (a–c) Voltage protocol and representative recordings of $ClC3_{13-19A}$, $ClC3_{13-19A}$ E281H, and $ClC3_{13-19A}$ E281Q. The insets represent enlarged the off-gating currents at the end of the voltage pulses. (d) Normalized nonlinear capacitance for ClC-3_{13-19A}, $ClC3_{13-19A}$ E281H, and $ClC3_{13-19A}$ E281Q. Inset shows enlarged the nonlinear capacitance of ClC-3_{13-19A}. Lines represent nonlinear fits to the data with the first derivative of a standard Boltzmann function. Fit parameters are presented in Table 1. (e) Current amplitudes of individual cells plotted against the corresponding off-gating charge Q_{off} (both at +135 mV) for ClC-3_{13-19A} WT, ClC-3_{13-19A} E281H, and ClC-3_{13-19A} E281Q (n = 8–13). Lines represent linear fits with zero origin to the data.

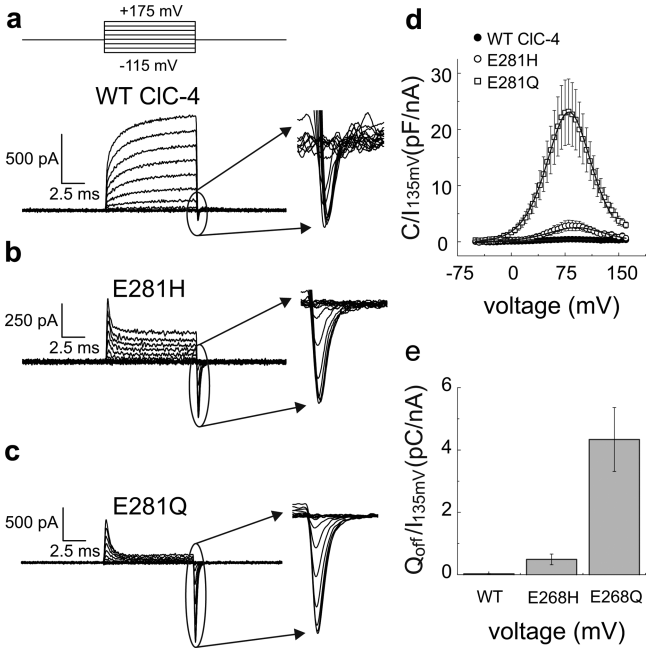

Figure 5. Gating charge and nonlinear capacitances of ClC-4. (a) Voltage protocol and representative current traces of ClC-4 WT and mutants. (b) ClC-4 E281H and (c) ClC-4 E281Q. Insets represent enlarged the corresponding off-gating currents at the end of the voltage pulses. (d) Normalized nonlinear capacitance for ClC-4 WT and E281H and E281Q. Lines represent nonlinear fits with the first derivative of a standard Boltzmann function. Fit parameters are presented in Table 1. (e) Ratio between ClC-4 off-gating charge (Q_{off}) and ionic currents at +135 mV (n = 7–8).

permits protonation and deprotonation exhibited an intermediate phenotype (Figure 5d, e). These findings demonstrate that ClC-4, similar to ClC-3 and ClC-5, is also capable of mediating nonlinear capacitances. Moreover, the proton glutamate E281 seems to play similar role in ClC-4 as in ClC-5[28] and to regulate the injection of protons from the internal aqueous solution into the protein.

In our functional studies of ClC-3, we used a modified construct in which a putative clathrin binding site at positions L13 to E19 was mutated (ClC-3_{13-19A}). To exclude the possibility that this alteration by itself might increase nonlinear capacitances, we generated the analogous construct: ClC-4_{13-19A} carrying a cluster of seven alanines at positions 13–19. This construct behaved similar to ClC-4 WT (Supporting Information Figure S3).

The Nonlinear Capacitances of ClC-3, ClC-4, and ClC-5 differ Significantly in Size and Voltage Dependence and Might Be Directly Involved in the Regulation of Luminal Acidification in Intracellular Compartments. Figures 1, S1, 4, and 5 show that the gating charge movements and nonlinear capacitances previously described for ClC-5[27,28] appear to be a characteristic feature for all mammalian ClC transporters. Figure 6b depicts a comparison of the relative nonlinear capacitances of ClC-3, ClC-4 and ClC-5 normalized to their ion transport amplitudes at +135 mV. Nonlinear capacitances were very small in ClC-4, but much bigger for ClC-3 and ClC-5. Whereas ClC-3 and ClC-4 displayed similar voltage dependences with a half-maximal voltage of activation ($V_{0.5}$ ~ +60 mV), the nonlinear capacitance of ClC-5 was shifted to more depolarizing potentials ($V_{0.5}$ ~ +110 mV) (Figure 6b).

To further illustrate the impact of the different voltage dependences, we employed a so-called envelope protocol (Supporting Information Figure S4) and quantified the mobilization of the gating charge in the E-to-Q exchanged proton glutamate mutants. All three isoforms exhibited similar kinetics (Figure 6c). However, at +90 mV only ~15% of the maximum charge could be mobilized for ClC-5, whereas the values for ClC-4 and ClC-3 were ~65% and ~82%, respectively. As a consequence, at less depolarized voltages, much higher capacitance changes are observed for ClC-3 than for the two other isoforms.

To estimate the effects of the membrane capacitance on vesicular acidification, we simulated intravesicular pH, [Cl^-] and the potential difference across the vesicle membrane for ClC proteins that are effective transporters such as ClC-4 or mainly capacitors as ClC-3. The calculations were performed closely following the methodology introduced by Rybak et al.[47] It uses a numerical solution of the equations describing the ionic distribution at equilibrium and is independent of the number of transporters and pumps in the vesicular membrane (see the Supporting Information). The endosomes are modeled as lipid spheres with different diameter and incorporated ATPases that pump protons into the vesicle lumen (Figure 6a). The proton pumps are the only primary active transport protein in

dx.doi.org/10.1021/cn400032z | ACS Chem. Neurosci. 2013, 4, 994–1003

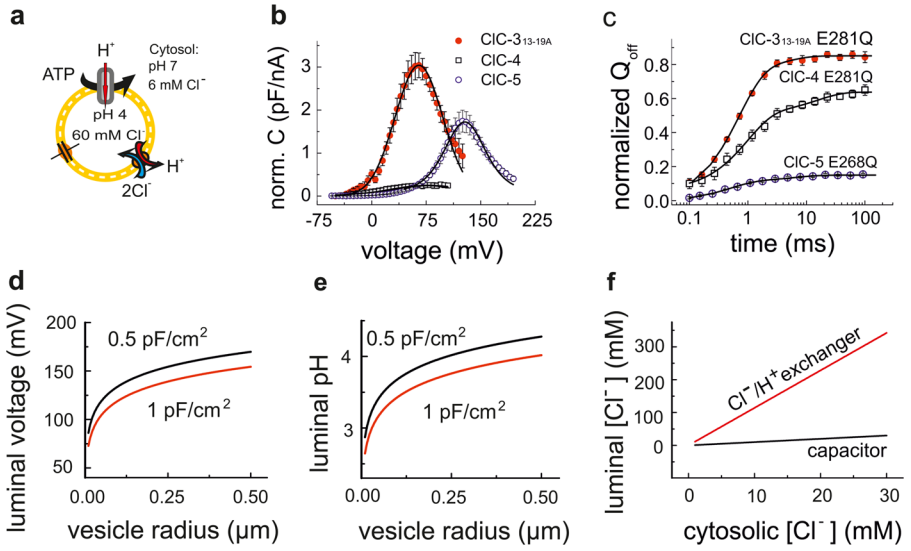

Figure 6. Functional specialization in mammalian ClC transporters (a) Schematic representation of the model system used for calculating intraendosomal pH and [Cl^-] depicting an intracellular vesicle with the corresponding ionic conditions and a ClC transporter that is operating either as coupled anion/proton exchanger or as capacitor. (b) Voltage dependence and amplitudes of the nonlinear capacitances of ClC-3_{13-19A}, ClC-4, and ClC-5 normalized to the corresponding ionic transport at +135 mV. (c) Kinetics of gating charge mobilization estimated using envelope protocols (Suppl. Figure S4) for the proton glutamate E-to-Q mutations in ClC-3_{13-19A}, ClC-4, and ClC-5. The off-gating charge (Q_{off}) following prepulses at +90 mV with different duration is normalized to the gating charge elicited by a reference pulse to +150 mV. (d, e) Estimated effects of the membrane capacitance on intravesicular potential and pH, respectively. Calculations were performed as described by Rybak et al.[47] with simulation parameters provided in the Supporting Information. (f) Dependence between intravesicular and cytosolic [Cl^-] calculated for vesicular ClC transporters functioning exclusively as capacitors or coupled exchangers.

the system and all passively built concentration gradients are coupled to the pH gradient established by this electrogenic transport process. As a consequence, the cumulative electrochemical gradient for all ions is limited by the energy provided by the hydrolysis of one molecule of ATP. [47]

Proton pumping automatically leads to an increase of the concentration of positive charges (protons) into the vesicular lumen and to more positive luminal electric potential. This creates a negative feedback loop that opposes efficient proton pumping by the V-type ATP-ases. The currently assumed role for ClC transport is to provide an electrical shunt and alleviate this effect by allowing negatively charged anions to pass the vesicular membrane and to decrease the positive potential of the vesicular lumen.[1] The observed large capacitance-to-transport proportion raises the question whether ClC-3 might modify vesicular acidification operating as a capacitor. Capacitance is the ability of a body to store electric charge and the charge that is stored in a capacitor is proportional to the applied voltage. Therefore, it is expected that larger membrane capacitances will result in lower intraendosomal voltage for a given pH gradient. To illustrate this interdependence, we modified the specific membrane capacitance in the mathematical model of vesicular acidification introduced above. Since we often observed nonlinear capacitances mediated by ClC proteins that exceeded the linear capacitance of the lipid membrane, we assumed that a 2-fold increase in vesicular capacitance is possible also under physiological conditions. The calculation predicted that such increase of the specific membrane capacitance (see Figure 6b) also leads to a reduction of the predicted positive intravesicular potential (Figure 6d). The lower electrical barrier for protons supports the acidification and result in lower steady-state luminal pH (Figure 6e). Therefore, ClC transporters can directly support acidification of intracellular compartments even when they function exclusively as capacitors. However, coupled transporters and capacitors have different effects on luminal chloride concentration (Figure 6f). [Cl^-] rises excessively when the ClC transporter function as Cl^-/H^+ antiporter, whereas an increased membrane capacitance without chloride conductance is expected to enhance exclusively luminal acidification.

DISCUSSION

Functional Properties of ClC-3. Our data present functional description and direct comparison of ClC-3, ClC-4, and ClC-5 and reveal significant similarities between these closely related isoforms. We showed that ClC-3 mediates coupled exchange of anions and protons across biological membranes, similarly to ClC-4 and ClC-5.[15,16] We also found that the three investigated isoforms exhibit at positive potentials nonlinear voltage dependent-capacitances. Moreover, we measured unitary transport rates for ClC-3 that are comparable to the unitary transport rates of ClC- 4 and ClC-5.[38,39] The nonstationary noise analysis revealed also that ClC-3, similarly to ClC-5, but not ClC-4, exhibits low transport probability.

The functional description of ClC-3 was accompanied with significant difficulties. For ClC-4 and ClC-5, heterologous expression results in surface insertion of a sufficient number of these transporters allowing functional characterization. [17] ClC-6 and ClC-7 can be studied electrophysiologically after removal of specific retention signals.[48,49] In contrast to the mentioned isoforms, conflicting functional data on ClC-3 have been published by several groups. The discrepancies are probably encountered because overexpression of ClC-3 does not result in insertion of a substantial number of transporters, but is rather associated with up-regulation of endogenous proteins. To overcome this problem, we increased the surface expression by mutating a previously identified retention signal or increased

dx.doi.org/10.1021/cn400032z | ACS Chem. Neurosci. 2013, 4, 994−1003

the nonlinear capacitances of ClC-3 by neutralizing the proton glutamate E281. The proton glutamate mutants,[27,28,37,38] resulted in defined alteration of ClC-3 function that closely resembled the effects of the homologous mutations in ClC-4 and ClC-5 (Figures 1, 3, and S1). The nonlinear capacitances obtained in this way do not occur in untransfected cells and in addition differ biophysically from the capacitances of the closely related ClC-4 and ClC-5. Therefore, they can be used to unambiguously discriminate currents by heterologously expressed ClC-3 from endogenous conductances and provide a compelling evidence that the here presented transport is mediated by this isoform. To finally ensure that the introduced N-terminal alternations in ClC-3_{13-19A} do not increase nonlinear capacitances per se, we inserted homologous mutations into ClC-4 but did not see such effects (Supporting Information Figure S3).

Two previous manuscripts report a functional description of ClC-3[21,50] that differ significantly from our results presented here. We suspect that recordings in these earlier papers might show currents generated by endogenous proton-activated anion conductance for the following reasons. In both publications, current amplitudes measured in untransfected and in ClC-3-transfected cells seem to be nearly identical. Second, endogenous proton activated currents in untransfected cells are also blocked by MTSES[21] but we did not observe such block for ClC-3_{13-19A}. Third, the capacitance of the cells shown in the experiments that have undergone silencing procedures[21] appears to be very high (~100 pF), which suggests that these procedures might have led to severe morphological changes. Large cell capacitances might have originated from enlarged cell surface which might strongly affect modification by MTS reagents. Finally, the authors used reversal potential measurements to determine the coupling stoichiometry of ClC-3. However, here measured chord conductances[51] did not differ between transfected and untransfected cells, indicating that reversal potential are substantially affected by endogenous transport proteins rendering equilibrium potential measurements for ClC-3 (but probably also for ClC-4 and ClC-5) unreliable.

Such reinterpretation of the results of the aforementioned two papers implies that ClC-3 might be required for the proper targeting of the ubiquitous proton-activated channels. Based on this hypothesis and on the effects on volume regulation,[7] one might postulate an important role of ClC-3 for the trafficking and cellular targeting of a variety of membrane proteins.

Physiological Importance of the Nonlinear Capacitances in Mammalian ClC Transporters. The functional characterization of ClC-3 revealed considerable similarities but also profound differences to ClC-4 and ClC-5. ClC-3, ClC-4, and ClC-5 all mediate coupled chloride/proton exchange and nonlinear capacitances (Figures 1–3).[15,16,27,28] In contrast, the voltage dependence, the transport probabilities and the size of nonlinear capacitances deviate strongly between the isoforms (Figure 6). These differences are unlikely to be caused by dramatically different underlying voltage sensing mechanisms, because the apparent unitary gating charge of the three proteins is very similar (Table 1). We recently demonstrated gating processes in ClC-5 that transform active into inactive transporters and vice versa. [28] Since nonlinear capacitances arise from incomplete transport cycles, ClC-3, ClC-4, and ClC-5 appear to differ in this particular gating process. Whereas a larger percentage of ClC-3 performs nontransporting cycles, ClC-4 appears to be specialized in mainly mediating ion transport. The specialization of the ClC isoforms might represent functional optimization in order to fulfill specific physiological requirements in distinct intracellular compartments. The capacitance of a cellular organelle determines the number of charges necessary to establish a certain membrane potential,[47] and thus plays crucial roles in shaping basic physiological processes like action potential generation and propagation. Computational analysis (Figure 6) suggests that insertion of a ClC protein into the membrane will increase the capacitance and thus limit the electrochemical barrier for protons and accordingly support luminal acidification. Moreover, expression of transport-incompetent ClC proteins will leave the luminal $[Cl^-]$ unaffected and permit differential regulation of luminal $[Cl^-]$ and $[H^+]$, for which distinct physiological roles have been demonstrated. [13]

ClC-3, ClC-4, and ClC-5 are localized in organelles with distinct properties (for a review see Jentsch[1]). Our data suggest that the different isoforms are also functionally specialized according to this distribution. ClC-3 is localized in very acidic organelles, like lysosomes and synaptic vesicles. *Clcn3* knockout mice exhibit reduced GABA-ergic synaptic transmission,[4] and hippocampus degeneration likely due to increased glutamate release.[3] Vesicular neurotransmitter transporters exhibit different dependencies on the chemical and electrical components of the H^+ electrochemical gradient. Whereas vesicular glutamate transporters are mainly driven by the vesicular membrane potential, GABA transporters utilize the chemical potential for protons to accumulate GABA.[52] In addition, vesicular physiology is strongly dependent and correlates to luminal $[Cl^-]$.[53−55] Our model predicts different effects on these three parameters (proton gradient, luminal potential and $[Cl^-]$) for different ClC transporters. ClC-3 acting as Cl^-/H^+ antiporter would result in high internal $[Cl^-]$ and consequently in excessive glutamate loading. On the contrary, ClC-3 acting predominantly as capacitor would permit effective acidification without profound chloride accumulation. It would therefore allow effective GABA accumulation, but restrict glutamate loading. ClC-5 resides mainly in endosomes, moderately acidified vesicles, and therefore might participate in both ion transport and electrical coupling. Cl^- accumulation in endosomes indeed depends on ClC-5 and is important for proper endocytosis.[13] ClC-4 may be localized to the endoplasmic reticulum,[56] characterized with neutral pH and absent proton electrochemical gradient. As a consequence, ClC-4 might be specialized mainly in ion transport in order to support ion homeostasis. All these considerations suggest that the here described functional specializations of ClC transporters provide flexible mechanisms for the differential regulation of luminal chloride concentration and pH in various intracellular compartments.

METHODS

Functional Expression. The DNA encoding the short guinea pig ClC-3 isoform (GeneBank U83464) with fused fluorescent protein mRFP at the C-terminus was inserted into the p156rrL vector using standard PCR. Similarly, human ClC-4 (GeneBank AB019432) together with an internal ribosome entry site (IRES) and a CD8 protein encoding sequence were inserted into the pRcCMV expression vector. A fluorescently tagged ClC-4 was also used, consisting of the monomeric fluorescent protein mCFP fused to the ClC-4 N-terminus into the pRcCMV vector. The construction of WT ClC-5 with the fluorescent protein mCherry fused to its C-terminus into the mammalian expression vector pRcCMV was described previously.[28] To remove the putative clathrin binding sites in ClC-3 and ClC-4, we

mutated all amino acids numbered from 13 to 19 to alanine using overlap extension PCR reaction. The point mutations E281Q, E281H in ClC-3 and ClC-4 and E268Q and E268H in the ClC-5 proteins were generated using QuikChange site-directed mutagenesis (Agilent Technologies). All mutants were verified by sequencing. HEK293T cells were cultured in DMEM medium (Invitrogen), supplemented with 10% fetal bovine serum (Biochrom AG) and 2 mM L-glutamine and 50 units/ml penicillin/streptomycin (Invitrogen). Cells were transiently transfected using Lipofectamine 2000 (Invitrogen).

Electrophysiology. Whole cell patch-clamp[57] was performed using an EPC-10 amplifier, software controlled by PatchMaster (HEKA Elektronik). Borosilicate pipettes (Harvard Apparatus) were pulled with resistances of 0.9−2 MΩ. Series resistance compensation and capacitance cancellation were applied, resulting in less than 5 mV voltage error. P/4 leak subtraction with a baseline potential of −30 mV was used to cancel linear capacitances. The standard external and internal recording solutions contained (in mM) 160 NaCl, 15 HEPES, 4 K KGluconate, 2 $CaCl_2$, 1 $MgCl_2$ and 105 NaCl, 15 HEPES, 5 $MgCl_2$, 5 EGTA, respectively. In all cases, 1% agar/3 M KCl salt bridges were used to connect the Ag/AgCl electrodes to the patch-clamp solutions.

Nonstationary Noise Analysis. Measurements were performed as described elswhere.[28] In brief, the external solution contained in mM: 145 NaSCN, 15 HEPES, 4 KGluconate, 2 CaGluconate, 1 MgGluconate, 0.1 NaCl; the internal solution contained in mM: 120 NaI, 20 HEPES, 2 MgGluconate, 5 EGTA, 0.1 NaCl, both adjusted to pH 7.4 with NaOH. Analysis was performed with PulseTools (HEKA). Variances were binned, and statistical deviations were superimposed as error bars. Background noise was measured at −40 mV and subtracted. Unitary transport rates (i) and the number of transporters in the membrane (N) were determined by plotting background-corrected variances (σ^2) against the mean current transport current (I) and fitting the following function to the data:

$$\sigma^2 = iI - \frac{I^2}{N}$$

Measurements of Membrane Capacitance. Membrane capacitance (C_m) was measured with the built-in software lock-in extension of PatchMaster (HEKA Elektronik). We used the sine-plus-DC technique[58] that utilizes the real and imaginary part of a sine wave signal plus the DC-conductance to determine the membrane capacitance, membrane conductance, and access resistance. The parameters used were as follows: sine wave at 800 Hz with 10 mV amplitude. The voltage dependence of the cell capacitance was measured by changing the voltage of the DC component. Nonlinear capacitances were plotted against the voltage and fitted with the first derivative of the standard Boltzmann function: [34]

$$C(V) = -Q_m \frac{zF\, e^{(zF(V-V_{0.5})/RT)}}{RT(1 + e^{(zF(V-V_{0.5})/RT)})^2}$$

with Q_m representing the maximum charge moved during the transition and $V_{0.5}$ being the half-maximal voltage of activation. In addition, the charge (z) denotes the apparent number of elementary charges (e_0) displaced over the membrane electric field. The equation contains in addition the universal gas constant (R), the Faraday constant (F), and the temperature (T).

Fluorescent Measurements of Intracellular pH. Fluorescent measurements of intracellular pH were performed as described previously.[28] Briefly, cells were loaded through the patch pipet with the pH-sensitive dye BCECF (2′,7′-bis-(2-carboxyethyl)-5-(and-6)-carboxy-fluorescein, Invitrogen) at a concentration of 37.5 μM. The buffer concentration (HEPES) in the pipet solution was 0.25 mM (osmolarity was adjusted by raising the [NaCl] to 120 mM). Measurements were performed on an inverted IX71 microscope (Olympus) equipped with UPlanSApo 60×/1.35 oil-immersion objective. The dye was excited sequentially at 440 and 490 nm using a Polychrome V fast-switching monochromator, and the fluorescence was detected at 530 nm using a PMT-equipped ViewFinder III (Till Photonics). Fluorescence ratios (F490/F440) were calculated and converted into absolute pH using a calibration curve obtained ex situ.

Confocal Imaging. Images were acquired 48−72 h after transfection at 1548 × 1548 pixels (145.30 × 145.3 nm), 16 bit intensity resolution with a Carl-Zeiss LSM 780 inverted microscope (Jena, Germany) using a 63×/1.40 DIC M27 oil immersion objective. The EGPF and EYFP (enhanced green and yellow fluorescence proteins) fluorophores were excited with a 488 nm argon laser; mRFP (monomeric red fluorescence protein) was excited with a 561 nm DPSS laser. The emitted signals were detected at 500−550, 520−560, and 560−650 nm, respectively. Cells were maintained during live cell imaging in PBS containing Ca^{2+} and Mg^{2+} (GIBCO) at room temperature (22−24 °C). Confocal images were assembled for publications using Carl Zeiss Zen lite 2011 (Blue edition) software (Carl Zeiss, Germany). In some cases, fluorescence images were superimposed on differential interference contrast (DIC) images taken simultaneously.

Data Analysis. Data analysis was performed using a combination of FitMaster (HEKA), Origin (OriginLab), SigmaPlot (Systat Software), and Excel (Microsoft) software. Summary data are presented as mean ± SEM.

■ ASSOCIATED CONTENT

Ⓢ Supporting Information

Four supplementary figures (Figures S1−S4) and information about the model of vesicular acidification. This material is available free of charge via the Internet at http://pubs.acs.org.

■ AUTHOR INFORMATION

Corresponding Author

*(A.K.K.) E-mail: alekov.alexi@MH-Hannover.de, alexi.alekov@gmail.com. Postal address: Medizinische Hochschule Hannover, OE4230, Carl-Neuberg-Str.1, D-30625 Hannover, Germany. Fax: ++49 511 532 2776. (Ch.F.) E-mail: c.fahlke@fz-juelich.de. Postal address: Institute of Complex Systems, Zelluläre Biophysik, Forschungszentrum Jülich, D-52425 Jülich, Germany.

Author Contributions

R.E.G., M.G., and A.K.K. performed the experiments and analyzed the data. R.E.G., M.G., Ch.F., and A.K.A. wrote the manuscript

Notes

The authors declare no competing financial interest.

■ ACKNOWLEDGMENTS

Dr. Gabriel Stölting for helpful suggestions.

■ ABBREVIATIONS

HEK293T, human embryonic kidney cells expressing the SV40 large T-antigen; WT, wild-type; YFP, yellow fluorescent protein; mRFP, monomeric red fluorescent protein; EGFP, enhanced green fluorescent protein; BCECF, 2′,7′-bis-(2-carboxyethyl)-5-(and-6)-carboxy-fluorescein; ATP, adenosine triphosphate

■ REFERENCES

(1) Jentsch, T. J. (2008) CLC Chloride Channels and Transporters: From Genes to Protein Structure, Pathology and Physiology. *Crit. Rev. Biochem. Mol. Biol. 43*, 3−36.

(2) Kawasaki, M., Uchida, S., Monkawa, T., Miyawaki, A., Mikoshiba, K., Marumo, F., and Sasaki, S. (1994) Cloning and expression of a protein kinase C-regulated chloride channel abundantly expressed in rat brain neuronal cells. *Neuron 12*, 597−604.

(3) Stobrawa, S. M., Breiderhoff, T., Takamori, S., Engel, D., Schweizer, M., Zdebik, A. A., Bösl, M. R., Ruether, K., Jahn, H.,

Draguhn, A., Jahn, R., and Jentsch, T. J. (2001) Disruption of ClC-3, a Chloride Channel Expressed on Synaptic Vesicles, Leads to a Loss of the Hippocampus. *Neuron 29*, 185−196.
(4) Riazanski, V., Deriy, L. V., Shevchenko, P. D., Le, B., Gomez, E. A., and Nelson, D. J. (2011) Presynaptic CLC-3 determines quantal size of inhibitory transmission in the hippocampus. *Nat. Neurosci. 14*, 487−494.
(5) Dickerson, L. W., Bonthius, D. J., Schutte, B. C., Yang, B., Barna, T. J., Bailey, M. C., Nehrke, K., Williamson, R. A., and Lamb, F. S. (2002) Altered GABAergic function accompanies hippocampal degeneration in mice lacking ClC-3 voltage-gated chloride channels. *Brain Res. 958*, 227−250.
(6) Britton, F. C., Hatton, W. J., Rossow, C. F., Duan, D., Hume, J. R., and Horowitz, B. (2000) Molecular distribution of volume-regulated chloride channels (ClC-2 and ClC-3) in cardiac tissues. *Am. J. Physiol.: Heart Circ. Physiol. 279*, H2225−2233.
(7) Xiong, D., Heyman, N. S., Airey, J., Zhang, M., Singer, C. A., Rawat, S., Ye, L., Evans, R., Burkin, D. J., Tian, H., McCloskey, D. T., Valencik, M., Britton, F. C., Duan, D., and Hume, J. R. (2010) Cardiac-specific, inducible ClC-3 gene deletion eliminates native volume-sensitive chloride channels and produces myocardial hypertrophy in adult mice. *J. Mol. Cell. Cardiol. 48*, 211−219.
(8) Wang, T., and Weinman, S. A. (2004) Involvement of chloride channels in hepatic copper metabolism: ClC-4 promotes copper incorporation into ceruloplasmin. *Gastroenterology 126*, 1157−1166.
(9) Mohammad-Panah, R., Wellhauser, L., Steinberg, B. E., Wang, Y., Huan, L. J., Liu, X.-D., and Bear, C. E. (2009) An essential role for ClC-4 in transferrin receptor function revealed in studies of fibroblasts derived from Clcn4-null mice. *J. Cell Sci. 122*, 1229−1237.
(10) Lloyd, S. E., Pearce, S. H. S., Fisher, S. E., Steinmeyer, K., Schwappach, B., Scheinman, S. J., Harding, B., Bolino, A., Devoto, M., Goodyer, P., Rigden, S. P. A., Wrong, O., Jentsch, T. J., Craig, I. W., and Thakker, R. V. (1996) A common molecular basis for three inherited kidney stone diseases. *Nature 379*, 445−449.
(11) Piwon, N., Günther, W., Schwake, M., Bösl, M. R., and Jentsch, T. J. (2000) ClC-5 Cl^--channel disruption impairs endocytosis in a mouse model for Dent's disease. *Nature 408*, 369−373.
(12) Hara-Chikuma, M., Wang, Y., Guggino, S. E., Guggino, W. B., and Verkman, A. S. (2005) Impaired acidification in early endosomes of ClC-5 deficient proximal tubule. *Biochem. Biophys. Res. Commun. 329*, 941−946.
(13) Novarino, G., Weinert, S., Rickheit, G., and Jentsch, T. J. (2010) Endosomal Chloride-Proton Exchange Rather Than Chloride Conductance Is Crucial for Renal Endocytosis. *Science 328*, 1398−1401.
(14) Smith, A. J., Reed, A. A. C., Loh, N. Y., Thakker, R. V., and Lippiat, J. D. (2008) Characterization of Dent's disease mutations of CLC-5 reveals a correlation between functional and cell biological consequences and protein structure. *Am. J. Physol.: Renal Physiol. 296*, F390−F397.
(15) Picollo, A., and Pusch, M. (2005) Chloride/proton antiporter activity of mammalian CLC proteins ClC-4 and ClC-5. *Nature 436*, 420−423.
(16) Scheel, O., Zdebik, A. A., Lourdel, S., and Jentsch, T. J. (2005) Voltage-dependent electrogenic chloride/proton exchange by endosomal CLC proteins. *Nature 436*, 424−427.
(17) Friedrich, T., Breiderhoff, T., and Jentsch, T. J. (1999) Mutational analysis demonstrates that ClC-4 and ClC-5 directly mediate plasma membrane currents. *J. Biol. Chem. 274*, 896−902.
(18) Zhao, Z., Li, X., Hao, J., Winston, J. H., and Weinman, S. A. (2007) The ClC-3 Chloride Transport Protein Traffics through the Plasma Membrane via Interaction of an N-terminal Dileucine Cluster with Clathrin. *J. Biol. Chem. 282*, 29022−29031.
(19) Duan, D., Winter, C., Cowley, S., Hume, J. R., and Horowitz, B. (1997) Molecular identification of a volume-regulated chloride channel. *Nature 390*, 417−421.
(20) Wang, X. Q., Deriy, L. V., Foss, S., Huang, P., Lamb, F. S., Kaetzel, M. A., Bindokas, V., Marks, J. D., and Nelson, D. J. (2006) CLC-3 Channels Modulate Excitatory Synaptic Transmission in Hippocampal Neurons. *Neuron 52*, 321−333.
(21) Matsuda, J. J., Filali, M. S., Collins, M. M., Volk, K. A., and Lamb, F. S. (2009) The ClC-3 Cl^-/H^+ Antiporter Becomes Uncoupled at Low Extracellular pH. *J. Biol. Chem. 285*, 2569−2579.
(22) Wang, L., Ma, W., Zhu, L., Ye, D., Li, Y., Liu, S., Li, H., Zuo, W., Li, B., Ye, W., and Chen, L. (2012) ClC-3 is a candidate of the channel proteins mediating acid-activated chloride currents in nasopharyngeal carcinoma cells. *Am. J. Physiol.: Cell Physiol. 303*, C14−C23.
(23) Nobles, M. (2004) Extracellular acidification elicits a chloride current that shares characteristics with ICl_{swell}. *Am. J. Physiol.: Cell Physiol. 287*, C1426−C1435.
(24) Lambert, S. (2005) Characterization of a proton-activated, outwardly rectifying anion channel. *J. Physiol. 567*, 191−213.
(25) Yamamoto, S., and Ehara, T. (2006) Acidic extracellular pH-activated outwardly rectifying chloride current in mammalian cardiac myocytes. *Am. J. Physiol.: Heart Circ. Physiol. 290*, H1905−1914.
(26) Wang, H.-Y., Shimizu, T., Numata, T., and Okada, Y. (2007) Role of acid-sensitive outwardly rectifying anion channels in acidosis-induced cell death in human epithelial cells. *Pflugers Arch. 454*, 223−233.
(27) Smith, A. J., and Lippiat, J. D. (2010) Voltage-dependent charge movement associated with activation of the CLC-5 $2Cl^-/1H^+$ exchanger. *FASEB J. 24*, 3696−3705.
(28) Grieschat, M., and Alekov, A. K. (2012) Glutamate 268 regulates transport probability of the anion/proton exchanger ClC-5. *J. Biol. Chem. 287*, 8101−8109.
(29) Zifarelli, G., De Stefano, S., Zanardi, I., and Pusch, M. (2012) On the mechanism of gating charge movement of ClC-5, a human Cl^-/H^- antiporter. *Biophys. J. 102*, 2060−2069.
(30) Armstrong, C. M., and Bezanilla, F. (1973) Currents Related to Movement of the Gating Particles of the Sodium Channels. *Nature 242*, 459−461.
(31) Holmgren, M., Wagg, J., Bezanilla, F., Rakowski, R. F., De Weer, P., and Gadsby, D. C. (2000) Three distinct and sequential steps in the release of sodium ions by the Na+/K+-ATPase. *Nature 403*, 898−901.
(32) Mager, S., Naeve, J., Quick, M., Labarca, C., Davidson, N., and Lester, H. A. (1993) Steady states, charge movements, and rates for a cloned GABA transporter expressed in Xenopus oocytes. *Neuron 10*, 177−188.
(33) Ashmore, J. F. (1990) Forward and reverse transduction in the mammalian cochlea. *Neurosci. Res. Suppl. 12*, S39−50.
(34) Santos-Sacchi, J. (1991) Reversible inhibition of voltage-dependent outer hair cell motility and capacitance. *J. Neurosci. 11*, 3096−3110.
(35) Li, X., Wang, T., Zhao, Z., and Weinman, S. A. (2002) The ClC-3 chloride channel promotes acidification of lysosomes in CHO-K1 and Huh-7 cells. *Am. J. Physiol.: Cell Physiol. 282*, C1483−1491.
(36) Fukuda, M. (1991) Lysosomal membrane glycoproteins. Structure, biosynthesis, and intracellular trafficking. *J. Biol. Chem. 266*, 21327−21330.
(37) Accardi, A., Walden, M., Nguitragool, W., Jayaram, H., Williams, C., and Miller, C. (2005) Separate ion pathways in a Cl^-/H^+ exchanger. *J. Gen. Physiol. 126*, 563−570.
(38) Zdebik, A. A., Zifarelli, G., Bergsdorf, E.-Y., Soliani, P., Scheel, O., Jentsch, T. J., and Pusch, M. (2008) Determinants of anion-proton coupling in mammalian endosomal CLC proteins. *J. Biol. Chem. 283*, 4219−4227.
(39) Alekov, A. K., and Fahlke, Ch. (2009) Channel-like slippage modes in the human anion/proton exchanger ClC-4. *J. Gen. Physiol. 133*, 485−496.
(40) Orhan, G., Fahlke, Ch., and Alekov, A. K. (2011) Anion- and proton-dependent Gating of ClC-4 anion/proton transporter under uncoupling conditions. *Biophys. J. 100*, 1233−1241.
(41) Picollo, A., Malvezzi, M., and Accardi, A. (2010) Proton block of the CLC-5 Cl^-/H^+ exchanger. *J. Gen. Physiol. 135*, 653−659.
(42) Heinemann, S. H., and Conti, F. (1992) Nonstationary noise analysis and application to patch clamp recordings. *Methods Enzymol. 207*, 131−148.

(43) Nguitragool, W., and Miller, C. (2006) Uncoupling of a CLC Cl-/H+ exchange transporter by polyatomic anions. *J. Mol. Biol. 362*, 682−690.
(44) Hebeisen, S., Heidtmann, H., Cosmelli, D., Gonzalez, C., Poser, B., Latorre, R., Alvarez, O., and Fahlke, Ch. (2003) Anion Permeation in Human ClC-4 Channels. *Biophys. J. 84*, 2306−2318.
(45) Alvarez, O., Gonzalez, C., and Latorre, R. (2002) Counting channels: a tutorial guide on ion channel fluctuation analysis. *Adv. Physiol. Educ. 26*, 327−341.
(46) Lingle, C. J. (2006) Empirical considerations regarding the use of ensemble-variance analysis of macroscopic currents. *J. Neurosci. Methods 158*, 121−132.
(47) Rybak, S. L., Lanni, F., and Murphy, R. F. (1997) Theoretical considerations on the role of membrane potential in the regulation of endosomal pH. *Biophys. J. 73*, 674−687.
(48) Neagoe, I., Stauber, T., Fidzinski, P., Bergsdorf, E.-Y., and Jentsch, T. J. (2010) The late endosomal ClC-6 mediates proton/chloride countertransport in heterologous plasma membrane expression. *J. Biol. Chem. 285*, 21689−21697.
(49) Leisle, L., Ludwig, C. F., Wagner, F. A., Jentsch, T. J., and Stauber, T. (2011) ClC-7 is a slowly voltage-gated $2Cl^-/1H^+$-exchanger and requires Ostm1 for transport activity. *EMBO J. 30*, 2140−2152.
(50) Matsuda, J. J., Filali, M. S., Volk, K. A., Collins, M. M., Moreland, J. G., and Lamb, F. S. (2008) Overexpression of CLC-3 in HEK293T cells yields novel currents that are pH dependent. *Am. J. Physol.: Cell Physiol. 294*, C251−C262.
(51) Hodgkin, A. L., and Huxley, A. F. (1952) The components of membrane conductance in the giant axon of Loligo. *J. Physiol. 116*, 473−496.
(52) Edwards, R. H. (2007) The Neurotransmitter Cycle and Quantal Size. *Neuron 55*, 835−858.
(53) Faundez, V., and Hartzell, H. C. (2004) Intracellular chloride channels: determinants of function in the endosomal pathway. *Sci. STKE 2004*, re8.
(54) Schenck, S., Wojcik, S. M., Brose, N., and Takamori, S. (2009) A chloride conductance in VGLUT1 underlies maximal glutamate loading into synaptic vesicles. *Nat. Neurosci. 12*, 156−162.
(55) Weinert, S., Jabs, S., Supanchart, C., Schweizer, M., Gimber, N., Richter, M., Rademann, J., Stauber, T., Kornak, U., and Jentsch, T. J. (2010) Lysosomal Pathology and Osteopetrosis upon Loss of H^+-Driven Lysosomal Cl^- Accumulation. *Science 328*, 1401−1403.
(56) Okkenhaug, H., Weylandt, K.-H., Carmena, D., Wells, D. J., Higgins, C. F., and Sardini, A. (2006) The human ClC-4 protein, a member of the CLC chloride channel/transporter family, is localized to the endoplasmic reticulum by its N-terminus. *FASEB J. 20*, 2390−2392.
(57) Hamill, O. P., Marty, A., Neher, E., Sakmann, B., and Sigworth, F. J. (1981) Improved patch-clamp techniques for high-resolution current recording from cells and cell-free membrane patches. *Pflugers Arch. 391*, 85−100.
(58) Gillis, K. D. (2000) Admittance-based measurement of membrane capacitance using the EPC-9 patch-clamp amplifier. *Pflugers Arch. 439*, 655−664.